Available online at www.sciencedirect.com
SCIENCE DIRECT®
Journal of Photochemistry and Photobiology A: Chemistry 171 (2005) 161–165
Journal of Photochemistry and Photobiology A:Chemistry
www.elsevier.com/locate/jphotochem

Self-assembly to prepare the ordered hexagonal mesostructured tin oxide/surfactant composite and its room temperature optical properties

Yude Wang[a,*], Ma Chunlai[b], Sun Xiaodan[b], Shuo Zhang[a], Hengde Li[b]

[a] *Department of Materials Science and Engineering, Yunnan University, Kunming 650091, People's Republic of China*
[b] *Department of Materials Science and Engineering, Tsinghua University, Beijing 100084, People's Republic of China*

Received 18 June 2004; received in revised form 12 August 2004; accepted 7 October 2004
Available online 13 November 2004

Abstract

Through self-assembly approach, tin oxide with an ordered hexagonal mesostructured tin oxide/surfactant composite (Sn–H) was synthesized in the presence of cationic surfactant (cetyltrimethylammonium bromide, CTAB: $CH_3(CH_2)_{15}N^+(CH_3)_3Br^-$) at room temperature. Powder X-ray diffraction (XRD) and transmission electron microscopy (TEM) results clearly showed the existence of ordered hexagonal mesostructure in the composite. According to the X-ray photoelectron spectroscopy (XPS) spectrum, the red-shift in the $3d_{5/2}$ peak position from the crystalline SnO_2 to the Sn–H composite indicates a change of microenvironments for tin, and this change is attributed to the interactions of surfactant CTAB with SnO_2. In comparison with SnO_2 bulk, the red-shift of the adsorption band of Sn–H composite can be clearly seen. The emission band of room temperature photoluminescence (RTPL) in the green spectral range was observed. The results obtained indicate that the interfacial effect between the tin oxide and the surfactants plays an important role in the optical properties.

Keywords: Ordered hexagonal mesostructure; Mesostructured tin oxide; Composite; Optical properties; Room temperature photoluminescence

1. Introduction

Tin oxide is an n-type semiconductor oxide with a wide-energy-gap (E_g = 3.6 eV, at 300 K). It is particularly interesting because it has semiconducting properties and has been widely used as a catalyst for oxidation of organic compounds, and as gas sensors [1,2], rechargeable Li-batteries [3,4], and optical electronic devices [5]. Owing to such a large range of applications, various methods have been applied for the synthesis of tin oxide. Beyond sample inorganic crystals, organic–inorganic composites are of further interest, since mesoscopic structures can be generated in the composite by replicating self-organized supramolecular assemblies of organic molecules [6]. In the past few years, mesostructured organic–inorganic composites arouse great recent interest from the viewpoints of both applications and fundamental research [7,8]. The primary goal is to combine the best properties of the inorganic phase with the best properties of the organic phase. Recent developments in the synthesis of self-assembled inorganic/organic surfactant composites have opened up a new field in the study of composite materials [9]. A novel chemical synthetic approach based on self-assembly between inorganic species and surfactant was presented to inorganic species and organic surfactant into two- and three-dimensional superlattice structures [10,11], and was successfully extended to numerous ordered inorganic–organic composites with nanometer scale periodicities [12,13]. The ordered tin oxide/surfactants mesostructure is a novel nanostructured semiconductor-surfactant superlattic materials that some novel properties could be thereby expected. However, among mesoporous materials, metal oxides/surfactant mesoporous composites with stability structure are relatively difficult to synthesize because of their multitude of different coordination numbers and oxidation states [14]. In this respect, several synthetic approaches utilizing the supramolecular templating mechanism had been reported for the preparation of mesoporous tin oxide [5,15–19] and some optical

* Corresponding author. Tel.: +86 871 5031410; fax: +86 871 5153832.
E-mail address: wangyude@tsinghua.org.cn (Y. Wang).

1010-6030/$ – see front matter © 2004 Elsevier B.V. All rights reserved.
doi:10.1016/j.jphotochem.2004.10.007

properties based on SnO_2 have been reported [20,21]. However, its room temperature photoluminescence feature, especially relative to the ordered mesoporous tin oxide, has rarely been mentioned and studied.

In this paper, an ordered hexagonal mesoporous tin oxide/surfactant composite (Sn–H) was synthesized, in which a cationic surfactant cetyltrimethylammonium bromide (CTAB) and simple chemical materials $SnCl_4{\cdot}5H_2O$ and tetramethylammonium hydroxide (TMAOH) at room temperature with self-assembly method, and unusual adsorption spectrum and novel room temperature photoluminescence (RTPL) of the resulted composite was observed.

2. Experimental

All the chemical reagents used in the experiments were obtained from commercial sources as guaranteed-grade reagents and used without further purification. The purities of $SnCl_4{\cdot}5H_2O$ and CTAB were 98 and 99%, respectively.

The synthesis method was based on the use of a cationic surfactant (CTAB) as structure directing agent, and hydrous tin chloride ($SnCl_4{\cdot}5H_2O$) as inorganic precursor and TMAOH as counterions, respectively. Reaction was performed at room temperature. The synthetic procedure was as follows: (1) 2.5 g CTAB were mixed with 26 ml distilled deionized water with stirring until a homogenous solution was obtained; (2) 36.45 g TMAOH (25 wt.% solution) was then added into the CTAB solution with stirring; (3) when the mixing solution became homogenous, a Sn^{4+} solution of 3.0 g $SnCl_4{\cdot}5H_2O$ diluted with 26 ml distilled deionized water was introduced, producing a white slurry; (4) after stirring 4 h, the product was aged at room temperature for 96 h; (5) the resulting product was filtered, washed with distilled water, dried at ambient temperature. For comparison, the as-synthesized product was extraction-treated with 100 ml ethanol for 1 h twice, and then filtered and washed with ethanol to remove the surfactant. This product was air-dried for 72 h.

As-synthesized product was characterized using Powder X-ray diffraction (XRD, Rigaku D/max-RB diffractometer with Cu Kα radiation λ = 1.5418 Å), transmission electron micrographs (TEM, Hitachi-800 transmission electron microscope operated at 200 KV), Fourier transformed infrared (FTIR) spectra (Perkin-Elmer Spectrum GX infrared spectrophotometer, the samples for FTIR were prepared using the KBr technology which were calibrated by polystyrene), X-ray photoelectron spectroscopy (XPS, Perkin-Elmer PHI 5300 ESCA). The optical properties were obtained with a UV2100 spectrophotometer and a HITACHI 850 type visible-ultraviolet spectrometer with a Xe laser as the excitation source.

3. Results and discussion

The typical low-angle X-ray diffraction (XRD) patterns for mesostructured tin inorganic/surfactant composite are shown in Fig. 1. The as-synthesized mesostructured tin oxide shows three diffraction peaks with lattice spacings d = 42, 24 and 21 Å. The diffraction peaks can be indexed as the (1 0 0), (1 1 0) and (2 0 0) reflections from two-dimensional hexagonal mesostructure with lattice constants a = 48.5 Å, as observed in typical XRD patterns of the hexagonal mesostructured silica MCM-41 [22,23]. The composite exhibits reflections of comparable integral intensity in the region 2θ 20–80° that are characteristic of cassiterite (inset of Fig. 1). The XRD patterns of sample as-synthesized and of the treated with ethanol are similar in intensity and position of peak. So the removal of the template by solvent extraction tends to preserve the mesostructure.

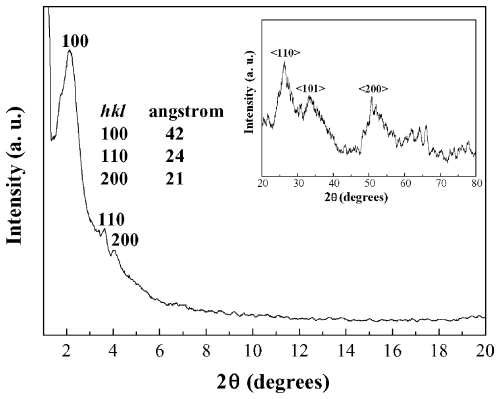

Fig. 1. Powder X-ray diffraction patterns for mesoporous Sn–H composite in low-angle and wide-angle range.

The appearance of low-angle diffraction peaks indicates that mesoscopic order is obtained in the Sn–H composite. This is confirmed by transmission electron microscopy (TEM) images. Fig. 2 shows TEM image of mesoporous Sn–H composite recorded along the [1 1 0] and [0 0 1] zone axes of the mesostructures. The mesoscopically ordered channels are readily observed to be arranged in hexagonal arrays by TEM. It is clear that the pore sizes are in the range of 24–26 Å and are uniform throughout the particles. The pore/channel walls are continuous and have thicknesses ∼2.2 nm. It is also consistent with the observed XRD patterns as discussed above. Fig. 2a shows characteristic image of Sn–H composite parallel to the pore channel axis (in the [0 0 1] direction) where the hexagonal mesostructure is clearly visible. Fig. 2b shows a view of Sn–H composite perpendicular to the pore axis in the [1 1 0] direction. Long, straight parallel tunnels are apparent in the image and the observed inter-pore distances are in good agreement with that obtained from the XRD patterns, Fig. 1.

The surface/near surface chemical composition of the sample analyzed by XPS is shown in Fig. 3a. The XPS spectrum of Sn–H composite shows two peaks of $3d_{5/2}$ and $3d_{3/2}$ at 486.6 and 494.9 eV with a better symmetry, and they are assigned to the lattice tin in tin oxide. They have peak separations of 8.3 eV between these two peaks. The values correspond to a 3d5 binding energy of Sn(IV) ion (indexed

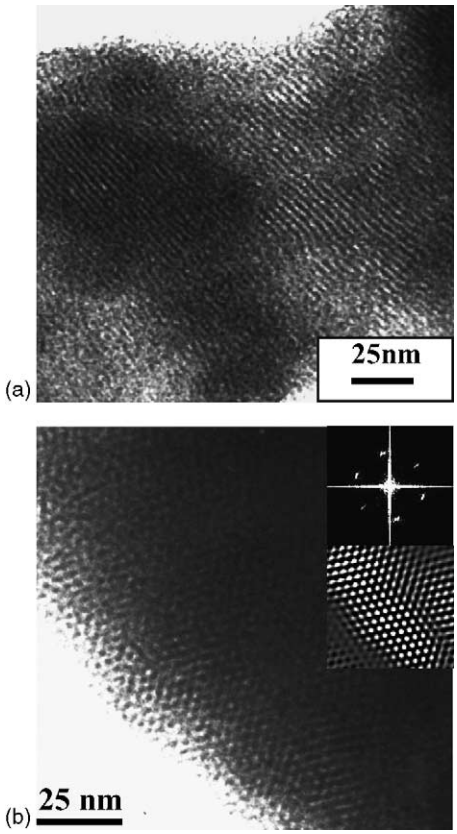

Fig. 2. TEM image of mesoporous Sn–H composite, (a) is recorded along the [1 1 0] zone axis and (b) alone the [0 0 1] zone axis, respectively. Inset in upper right, optical Fourier transform of the part image.

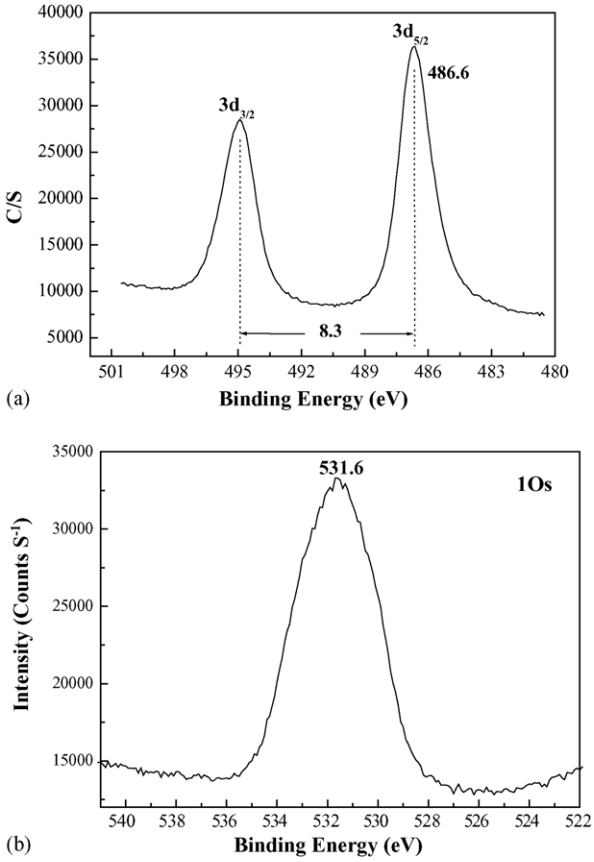

Fig. 3. XPS spectrum of Sn–H composite: (a) Sn 3d and (b) O 1s.

Standard ESCA Spectra of the Elements and Line Energy Information, Φ Co., USA). The red-shift in the $3d_{5/2}$ peak position from the crystalline SnO_2 (Sn–H composite calcined at 500 °C for 2 h) to the Sn–H composite (from 487.5 to 486.6 eV) indicates a change of microenvironments for tin. This shift (0.9 eV) is due to the interaction of surfactant CTAB with SnO_2. This red-shift results have been observed in mesoporous titania by the Ozin [24] and Zaban groups [25]. In Fig. 3b, it can be seen that the O1s XPS is asymmetric (the left side is little wider than that of the right), indicating that at least two kinds of oxygen species were present in the near surface region. The peak at about 531.6 eV is due to the SnO_2 crystal lattice oxygen, while the peak at about 533 eV is due to chemisorded oxygen.

UV–vis spectroscopy was used to characterize the optical absorbance of Sn–H composite. The absorption and corresponding band gap energy of SnO_2 bulk are $\lambda = 350$ nm and $E_g = 3.6$ eV. Fig. 4 shows the UV–vis absorption spectrum of Sn–H composite. It can be seen that there is a strong band edge absorption in the spectrum region of longer than 350 nm in wavelength. It is well known that the absorption coefficient of an amorphous semiconductor has a characteristic relation [26]: $[\alpha\eta\omega]^{1/2} = A[\eta\omega - E_g]$, in which $\eta\omega$ is the photon energy, E_g the apparent optical band gap, A the constant characteristic of the amorphous semiconductor, and α the absorption coefficient. Therefore, the E_g of Sn–H composite can be obtained by the extrapolation of the above relation to be 2.24 eV (see Fig. 4 inset). A red-shift of approximately 1.36 eV relative to bulk SnO_2 is evident for the Sn–H composite. This is contrary to the quantum size effect which leads to the blue-shift of E_g with decrease of particle size, which has been observed in many nanometer-sized semiconductor materials [27]. The red-shift of absorption spectrum or appeared optical

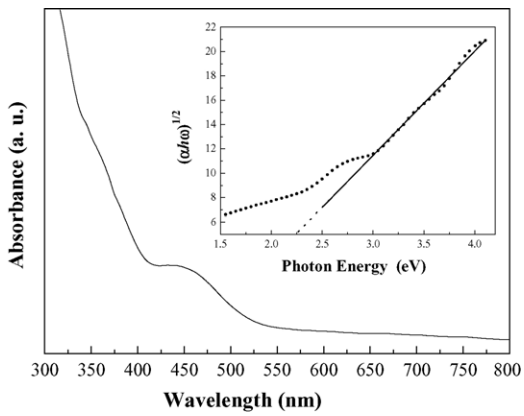

Fig. 4. The absorbance spectra and the apparent energy gap (inset) of Sn–H composite from the extrapolation of Urbach's equation.

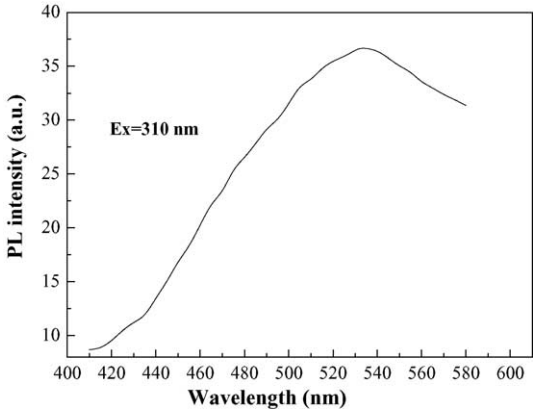

Fig. 5. Photoluminescence spectrum of Sn–H composite recorded at room temperature by excitation 310 nm.

band gap is worthy to point out that this different would arise from the interface between tin oxide and surfactant. However, the sample of these treated with ethanol does not show the red-shift.

In our investigation, room temperature photoluminescence spectra were performed with an excitation wavelength (λ_{ex} = 310 nm). The RTPL spectrum of tin oxide/surfactant mesophase is shown in Fig. 5. The RTPL spectrum exhibits a broad emission band between 440 and 580 nm, centered at 534 nm. When compared to the SnO_2 nanoribbons, the photoluminescence from the tin oxide/surfactant mesostructure is red-shifted. However, for the sample of these treated with ethanol, any spectrum of room temperature photoluminescence was not observed.

Charge density matching between the surfactant and the inorganic species was important for the formation of the organic–inorganic mesophases [28]. Huo and co-workers proposed a generalized mechanism of formation based on the specific type of electrostatic interaction between a given inorganic precursor I and surfactant head group S [29]. By extension, another charge-interaction pathway was $S^+ X^- I^+$, where S^+ was the structure director, I^+ was the inorganic precursor and X^- was a counterion. We suggested that this pathway could explain the formation of the mesostructure tin oxide. Under acidic conditions, through the $S^+ X^- I^+$ pathway the cationic tin species (I^+) and the surfactant templating agent CTA^+ (S^+) could be used to synthesize mesostructured tin oxide. The X^- (halide anions such as Cl^- and Br^-, and OH^-) became involved through this pathway as it served to buffer the repulsion between the S^+ and I^+ by means of weak hydrogen-bonding forces. The interactions between the surfactant molecules (CTA^+) and the inorganic counterions (OH^-) can postpone the combination of the inorganic ions, and the self-assembling of inorganic materials and surfactant molecules will prefer to happen so as to form a mesophase through hydrogen-bonding interactions. According to our mechanism, OH^- should might self-assemble around the cationic surfactant (CTAB) molecules before the addition of the Sn^{4+} solution so that the Sn^{4+} ions can be attracted by the assembled OH^- to form the mesostructured tin oxide.

It was reported recently that SnO_2 nanocrystalline thin films has only a broad dorminant photoemission peak at 396 nm (3.13 eV) at 300 K [30]. For the SnO_2 nanoribbons, there are two strong peaks at 392 (3.2 eV) and 439 nm and two weak peaks at 489 and 496 nm at the room temperature [31]. The photoluminescence was attributed to the donor–acceptor pair transitions or to the luminescent center, such as nanocrystals and defects caused by impurities during the growth, but that is not yet clear [18,19]. To the best of our knowledge, it is difficult to observe any photoluminescence phenomenon at room temperature for bulk SnO_2 [32]. The mesostructured tin oxide/surfactant composites show well-defined ordered structure to form tin oxide/surfactant superlattices. This peculiar structure might have a profound effect on the chemical and physical properties of tin oxide. Some SnO_2 nanoparticles capped with stearic acid has been reported to exhibit unusual room temperature photoluminescence [27]. We think that the interfacial effect of tin oxide/surfactants composite between tin oxide and the organic surfactants might be similar to the nanoparticles coated with stearic acid reported by Wu et al. [27]. A great lot of oxygen vacancies mainly located on the interface of inorganic framework have interactions with interfacial capping surfactants, and surfactants might stabilize *F*-center-like oxygen vacancies. These interactions will lead to form the trapped state that might form a series of metastable energy levels within the band gap. The metastable energy levels are relatively long lifetime and their optical transitions are dipole allowed. So, the room temperature photoluminescence can be observed. Therefore, it could be inferred that the room temperature photoluminescence of tin oxide/surfactants mesophase might be induced by the interfacial effects between the inorganic framework and the surfactants.

4. Conclusions

SnO_2/surfactant inorganic–organic nanocomposites with ordered hexagonal mesostructure were synthesized based on self-assembly between a cations surfactant (CTAB) and a sample inorganic precursor ($SnCl_4 \cdot 5H_2O$). The prepared nanocomposites were characterized by X-ray diffraction (XRD), transmission electron micrographs (TEM) and X-ray photoelectron spectroscopy (XPS). The optical absorption and photoluminescence spectra have been measured. It has been found that SnO_2/surfactant composites have a significant red-shift of the optical absorption band edge and appeared optical band gap in contrast to that bulk SnO_2, and an unusual room temperature photoluminescence (RTPL). The results obtained indicate that the interfacial effect between the tin oxide and the surfactant plays an important role in the optical properties.

Acknowledgements

We thank Y. Fu for help with emission spectroscopy measurements and X.Y. Ye with XPS measurements. This work was supported by the Key Project of Chinese Ministry of Education, the Natural Science Foundation of Yunnan Province, China (No. 2002E0004Q), and the Project of Yunnan University for Science and Engineering (No. 2003Z003A).

References

[1] C. Nayral, T. Ould-Ely, A. Maisonnat, B. Chaudret, P. Fau, L. Lescouzeres, A. Peyre-Lavigne, Adv. Mater. 11 (1999) 61–63.
[2] E.R. Leite, I.T. Weber, E. Longo, J.A. Varela, Adv. Mater. 12 (2000) 965.
[3] A.S. Yu, R. Frech, J. Power Source 104 (2002) 97–100.
[4] S.C. Nam, Y.S. Yoon, W.I. Cho, B.W. Cho, H.S. Chun, K.S. Yun, Electrochem. Commun. 3 (2001) 6–10.
[5] F.L. Chen, M.L. Liu, Chem. Commun. (1999) 1829–1830.
[6] H. Sugimura, A. Hozumi, T. Kameyama, O. Katai, Adv. Mater. 13 (2001) 667–670.
[7] S. Mann, G.A. Ozin, Nature 382 (1996) 313–318.
[8] W. Shenton, D. Pum, U.B. Sleytr, S. Mann, Nature 389 (1997) 585–587.
[9] S.H. Tolbert, P. Sieger, G.D. Stucky, S.M.J. Aubin, C.C. Wu, D.N. Hendrickson, J. Am. Chem. Soc. 119 (1997) 8652–8661.
[10] Q.S. Huo, D.I. Margolese, U. Ciesla, D.G. Demuth, P. Feng, T.E. Gier, P. Sieger, A. Firouzi, B.F. Chmelka, F. Schuth, G.D. Stucky, Chem. Mater. 6 (1994) 1176–1191.
[11] G.D. Stucky, Q.S. Huo, A. Firouzi, B.F. Chmelka, SchachtF S., I.G. Voigt-Martin, F. Schuth, Stud. Surf. Sci. Catal. 105 (1996) 3, 28 Part A–C.
[12] A. Sayari, P. Liu, Micoporous. Mater. 12 (1997) 149–177.
[13] W.Y. Lin, W.Q. Peng, J.Z. Sun, J.C. Shen, J. Mater. Chem. 9 (1999) 641–642.
[14] X.D. Sun, C.L. Ma, Y.D. Wang, H.D. Li, Mater. Lett. 54 (2002) 244–247.
[15] N. Ulagappan, C.N.R. Rao, Chem. Commun. (1996) 1685–1686.
[16] L.M. Qi, J.M. Ma, H.M. Cheng, Z.G. Zhao, Langmuir 14 (1998) 2579–2581.
[17] K.G. Severin, T.M. Abdel-Fatlah, T.J. Pinnavaia, Chem. Commun. (1998) 1471–1472.
[18] J.Y. Ying, C.P. Mehnert, M.S. Wong, Angew. Chem. Int. Ed. Engl. 38 (1999) 56–77.
[19] Y.D. Wang, C.L. Ma, X.D. Sun, H.D. Li, Microporous Mesoporous Mater. 49 (2001) 171–178.
[20] J.Q. Hu, X.L. Ma, N.G. Shang, Z.X. Xie, N.B. Wong, C.S. Lee, S.T. Lee, J. Phys. Chem. B 106 (2002) 3823–3826.
[21] T.W. Kim, D.U. Lee, Y.S. Yoon, J. Appl. Phys. 88 (2000) 3759–3761.
[22] C.T. Kresge, M.E. Leonowicz, W.J. Roth, J.C. Vartuli, J.S. Beck, Nature 359 (1992) 710–712.
[23] J.S. Beck, J.C. Vartuli, W.J. Roth, M.E. Leonowicz, C.T. Kresge, K.D. Schmitt, C.T.W. Chu, D.H. Olson, E.W. Sheppard, S.B. McCullen, J.B. Higgins, J.L. Schlenker, J. Am. Chem. Soc. 114 (1992) 10834–10843.
[24] D. Khushalani, G.A. Ozin, A. Superman, J. Mater. Chem. 9 (1999) 1491–1500.
[25] Y.Q. Wang, S.G. Chen, X.H. Tang, O. Palchik, A. Zaban, Y. Tolypin, A. Gedanken, J. Mater. Chem. 11 (2001) 521–526.
[26] G. Mills, Z.G. Li, D. Mersel, J. Phys. Chem. 92 (1988) 822–828.
[27] X.C. Wu, B.S. Zou, J.R. Xu, B.L. Yu, G.Q. Tang, G.L. Zhang, W.J. Chen, Nanostruct. Mater. 8 (1997) 179–189.
[28] P.D. Yang, D.Y. Zhao, D.I. Margolese, B.F. Chmelka, G.D. Stucky, Chem. Mater. 11 (1999) 2813–2826.
[29] Q.S. Huo, D.I. Margolese, U. Ciesla, P. Feng, T.E. Gier, P. Sieger, R. Leon, P.M. Petroff, F. Schuth, G.D. Stucky, Nature 368 (1994) 317–321.
[30] T.W. Kim, D.U. Lee, J.H. Lee, D.C. Choo, M. Jung, Y.S. Yoon, J. Appl. Phys. 90 (2001) 175–180.
[31] J.Q. Hu, X.L. Ma, N.G. Shang, Z.Y. Xie, N.B. Wong, C.S. Lee, S.T. Lee, J. Phys. Chem. B 106 (2002) 3823–3826.
[32] M.D. Murcia, M. Egee, J.P. Fillard, J. Phys. Chem. Solids 39 (1977) 629–635.